ISPRS Journal of Photogrammetry and Remote Sensing 153 (2019) 96–109

Contents lists available at ScienceDirect

ISPRS Journal of Photogrammetry and Remote Sensing

journal homepage: www.elsevier.com/locate/isprsjprs

Innovative pheno-network model in estimating crop phenological stages with satellite time series

Chunyuan Diao

Department of Geography and Geographic Information Science, University of Illinois at Urbana-Champaign, Urbana, IL 61801, USA

ARTICLE INFO

Keywords:
Complex network
Time series
Optical imaging
Phenology
Agriculture

ABSTRACT

Large-scale remote monitoring of crop phenological development is vital for scheduling farm management activities and estimating crop yields. Tracking crop phenological progress is also crucial to understand agricultural responses to environmental stress and climate change. During the past decade, time series of remotely sensed imagery has been increasingly employed to monitor the seasonal growing dynamics of crops. A variety of curve-fitting based phenological methods have been developed to estimate critical phenological transition dates. However, those phenological methods are typically parametric by making mathematical assumptions of crop phenological processes and usually require year-long satellite observations for parameter training. The assumption and constraint make those methods inadequate for phenological monitoring in heavy cloud-contaminated regions or in complex agricultural systems. The objective of this study is to estimate crop phenological stages with satellite time series using a complex network-based phenological model (i.e., "pheno-network"). The innovative pheno-network model is non-parametric without mathematically defined phenological assumptions and can be constructed with partial-year remote sensing data. Rooted in network theory, the pheno-network model characterizes the complex phenological process with spectrally defined nodes and edges. It provides an innovative network representation to model the temporal dynamics of spectral reflectance of crops throughout the growing season. With corn and soybean in Illinois as a case study, the pheno-network model was devised to estimate their phenological transition dates along the leaf senescence trajectory from 2002 to 2017. Results indicated that the estimated transition dates of corn had strong correlation with its ground-observed mature stage. As for soybean, the estimated transition dates were closely associated with its dropping leaves stage. The pheno-network model shows marked potential to advance phenological monitoring in complex agricultural diversified and intensified systems.

1. Introduction

Vegetation phenology, as the recording of seasonally recurring events (e.g., leaf emergence and senescence), has been long studied to characterize the ecosystem structures and functions (Lieth, 2013). The phenological dynamic of vegetation over the course of a year regulates the terrestrial gross primary productivity, biogeochemical cycling, and water-energy-carbon fluxes (Morisette et al., 2008; Peñuelas and Filella, 2001). It has been increasingly utilized in parameterizing climate models, hydrological models, and terrestrial biosphere models to improve the understanding of biosphere-atmosphere-hydrosphere interactions (Foley et al., 2000; MacBean et al., 2015; Richardson et al., 2012). This seasonal dynamic of vegetation is also a sensitive indicator of vegetation response to global climate and environmental changes (Kramer et al., 2000; Richardson et al., 2013). To understand the mechanisms driving the phenological process and its subsequent feedback to earth systems, tracking the vegetation growth along the phenological trajectory is essentially crucial.

Among a range of terrestrial ecosystems, phenological monitoring in agriculture is particularly important. The growth and development stages of crops are closely associated with various management activities (e.g., fertilizer and irrigation scheduling), and have considerable implications for yield estimation (Sakamoto et al., 2013; Walthall et al., 2013; Zhang and Zhang, 2016). The crop requirement of resources (e.g., water and nutrient) varies along the phenological trajectory. Its response to climate change and environmental stress also differs (Brown et al., 2012; Gao et al., 2017). For instance, the silking stage of corn is particularly sensitive to drought stress, as drought may cause poor pollination and sterility of corn and a subsequent decrease in corn yield (Lauer, 2012). The setting pods stage of soybean is sensitive to environmental stress (e.g., moisture and high temperature) with regard to the yield reduction (Kilgore and Fjell, 1997). The crop phenological

E-mail address: chunyuan@illinois.edu.

https://doi.org/10.1016/j.isprsjprs.2019.04.012
Received 17 December 2018; Received in revised form 20 April 2019; Accepted 20 April 2019

progress also constitutes a key component in crop simulation models for predicting the yields (Bolton and Friedl, 2013; Jin et al., 2017; Lobell et al., 2015), and in operational crop mapping (Dong and Xiao, 2016; Gómez et al., 2016; Qin et al., 2015; Wang et al., 2017; Zhong et al., 2016). Large-scale monitoring of crop phenological development in a rapid, consistent, and repeated fashion is indispensably a critical step towards assessing the agricultural response to future climate change and increasingly growing population.

The increasing availability of earth observation satellites, along with the technical advancements in remotely sensed imagery processing, has facilitated the remote tracking of phenological development of vegetation over wide geographical regions through time (Diao and Wang, 2016a, 2018; Liu et al., 2017; White et al., 1997). Time series of remotely sensed imagery acquired over the course of a year is employed to characterize the crop phenophases and to capture the critical phenological transition dates (e.g., onset, end, and length of growing season) (Boschetti et al., 2009; Gao et al., 2017; Manfron et al., 2017; Sakamoto et al., 2005; Wardlow et al., 2006). Over the past decade, a suite of curve-fitting based phenological methods have been developed, including double logistic methods, wavelet methods, harmonic methods, two-step filtering methods, asymmetric Gaussian methods, and high-order spline methods (Beck et al., 2006; Diao and Wang, 2014; Hermance et al., 2007; Jonsson and Eklundh, 2002; Moreira et al., 2019; Sakamoto et al., 2010; Sakamoto et al., 2005; Zhang et al., 2003). With those phenological methods, the remotely sensed greenup onset of the growing season has been found to be closely associated with the ground-observed emergence stage of crops. The remotely retrieved dormancy onset has been indicated to be related to the field-observed harvest stage of crops (Gao et al., 2017; Wardlow et al., 2006). Despite the promising detection results, those phenological methods are typically parametric by assuming that the process of phenological development can be modeled by defined mathematical equations (e.g., logistic functions). They usually require year-long satellite observations for parameter training and optimization. Affected by a combination of natural and anthropogenic factors, the increasing agricultural diversification and intensification complicate the phenological signal captured by the satellites. The phenological process in those complex systems might not be adequately modeled by defined mathematical forms (Atkinson et al., 2012). Besides, the satellite observations may be contaminated by cloud and atmospheric aerosols to varying degrees, which can make the acquisition of year-long remotely sensed data challenging, particularly in tropical and high latitude regions.

The recent advance in network science opens up new opportunities to model various complex systems (Barabási, 2009; Newman et al., 2011). Rooted in network theory, complex networks characterize the sophisticated relationships between constituents of systems with collections of nodes and edges, such as social networks, biological networks, and narrative networks (Brockmann and Helbing, 2013; Buldyrev et al., 2010; Eagle et al., 2009; Rubinov and Sporns, 2010; Watts and Strogatz, 1998). The nodes are defined as the objects of interest in complex systems, and the edges define the interactions between those objects. It provides an abstract representation of complex systems by capturing the fundamental structures and patterns (Newman, 2010). Complex networks have been actively explored in a multitude of fields, ranging from biological to social sciences. The flexibility of defining the nodes and edges in complex networks provides a wealth of possibilities to understand the complicated phenomena, which may shed light on the aforementioned phenological challenges with remote sensing imagery. Yet complex networks have seldom been studied in remote sensing to represent the massive information contained by time series of satellite imagery. Its potential to model the complex remotely sensed phenological process, particularly in agricultural systems, is to be explored.

The objective of this study is to estimate the crop phenological stages with partial satellite time series using a complex network-based phenological model (i.e., “pheno-network”). The pheno-network model tracks the temporal changes of spectral reflectance of agricultural crops across the phenological development stages, with an innovative network-based representation. Specifically, this study is designed to capture the critical phenological transition dates when the agricultural crops shift from green leaf-dominating growth stages to the soil-dominating harvest stage along the leaf senescence trajectory, through uncovering the underlying structures of relationships of spectral reflectance across corresponding phenological stages. As a case study, the pheno-network model is applied to the partial time series of Moderate Resolution Imaging Spectroradiometer (MODIS) to remotely estimate the mature stage of corn and the dropping leaves stage of soybean in Illinois from 2002 to 2017.

2. Study site and data

2.1. Study site

The study site is the state of Illinois in the Midwestern US, which covers an area of 150,000 km^2. It is lying within the Central Plains, characterized by relatively flat topography. The climate in most of Illinois is humid continental, with hot humid summers and cold snowy winters. The average annual rainfall is over 48 in. in the southern Illinois, and around 35 in. in the north. Illinois is a major agricultural state in the US Corn Belt region, and ranks among the top in corn and soybean production. It is partitioned into nine agricultural statistics districts (ASDs) according to climate, geography, and cropping practices (Fig. 1). These nine ASDs are northwestern (NW), northeastern (NE), western (W), central (C), eastern (E), west southwestern (WSW), east southeastern (ESE), southwestern (SW), and southeastern (SE) districts. As two predominant crop types, corn and soybean are

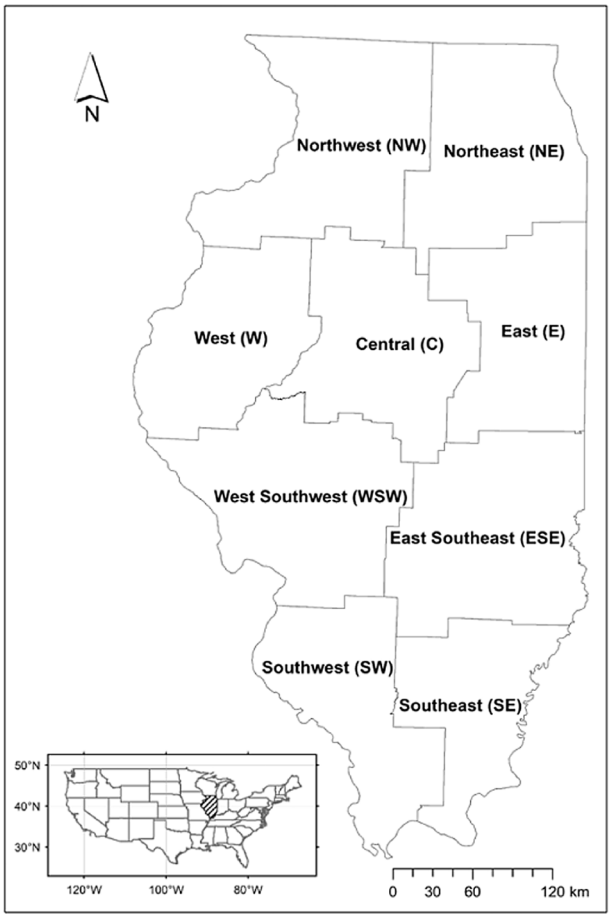

Fig. 1. Nine agricultural statistics districts (ASDs) of Illinois.

typically rotated in consecutive years. According to United States Department of Agriculture (USDA) National Agricultural Statistics Service (NASS), there are six phenological development stages for corn and soybean, respectively. The phenological stages for corn are emerged, silking, dough, dent, mature, and harvest stages. The phenological stages for soybean are emerged, blooming, setting pods, turning yellow, dropping leaves, and harvest stages.

2.2. Data

2.2.1. MODIS data and pre-processing

The MODIS Nadir Bidirectional reflectance distribution function Adjusted Reflectance (NBAR) data (MCD43A4, version 6), acquired from Land Processes Distributed Active Archive Center (LP DAAC), were used in this study to construct the pheno-network model. The MCD43A4 data are daily 16-day composite imagery, with a spatial resolution of 500 m. At each date, the surface reflectance is composited during a 16-day retrieval period (including its eight preceding days and seven following days) using all the imagery from both Terra and Aqua sensors. This composite imagery reduces the influence of atmospheric aerosols, illumination differences, and cloud contamination. To take into account solar and viewing geometries, the MCD43A4 data employ the bidirectional reflectance distribution function (BRDF) correction algorithm to normalize the surface reflectance under a nadir view. Compared to other satellite-based observations, this high temporal resolution and BRDF-corrected imagery is more appropriate to construct the time series throughout the year to track the crop phenological progress. The MCD43A4 data covering the Illinois from 2002 to 2017 were acquired in this study. Seven bands (bands 1–7) that are characteristic of crop properties (e.g., chlorophyll content, water content, and leaf cell structure) were taken as the spectral reflectance in the pheno-network model.

To further diminish the influence of atmospheric interference and noise, the MCD43A4 data were pre-processed with ancillary quality assurance layers. First, the MCD43A4 data were filtered using the snow/ice quality layer of the MODIS BRDF/Albedo Quality data (MCD43A2, version 6). As snow and ice may cause abnormal and outlying spectral reflectance values in the data, this quality assurance layer was used to filter out the pixels of each observation date that were subject to snow/ice contamination. Second, the MCD43A4 data were further pre-processed using the MODIS land surface temperature (LST) data (MOD11A1, version 6). Corn and soybean are typically harvested before the winter season. The daytime surface skin temperature layer of the MODIS LST data was employed to identify the winter period when snow might occur. For each acquisition date, the pixels with the daytime LST values lower than 5 °C were flagged as spurious spectral values (Zhang et al., 2006). Those invalid or missing observations, identified by quality assurance layers, were then replaced by the moving average of the surrounding closest good quality neighbors in the time series of the MCD43A4 data. After the pre-processing, only the downward period of the time series was retained for each pixel, as the pheno-network model was to be built with the partial-year data. The downward period denotes the temporal trajectory when the normalized difference vegetation index (NDVI) of the pixel has a decreasing trend in the time series. The downward period is also taken as the leaf senescence trajectory of crops in this study. The pheno-network model was constructed in this downward period to estimate the critical phenological transition dates when the agricultural crops shift from green leaf-dominating growth stages to the soil-dominating harvest stage, namely the mature stage of corn and the dropping leaves stage of soybean.

2.2.2. Reference data

Two predominant crop types in Illinois are corn and soybean. According to Cropland Data Layer (CDL) in 2017, corn was grown in about 31% of the land in Illinois, and soybean was planted in 28% of Illinois. The CDL data are generated by USDA on an annual basis using the remotely sensed imagery to map the distribution and extent of major crop types in the US (Johnson and Mueller, 2010). In Illinois, the remote sensing data for deriving CDL are mainly from the Landsat, the Disaster Monitoring Constellation (DMC) DEIMOS-1 and UK2, the Indian Space Research Organization (ISRO) ResourceSat-1 Advanced Wide Field Sensor (AWiFS), ResourceSat-2 LISS-3, and the Sentinel-2 sensors. The CDL data are produced using the decision tree classifier or maximum likelihood classifier at a spatial resolution of 30 m (or 56 m), with high accuracy achieved for both corn and soybean classes in Illinois. The producer's accuracies and user's accuracies for both classes are higher than 90% for most of the years. In this study, the CDL data were resampled to the spatial resolution of the MCD43A4 data (i.e., 500 m) and the fractions of corn and soybean were calculated for each resampled pixel. At 500 m spatial resolution, the phenology recorded by satellites may be affected by the mixture of multiple land covers, and may not correspond to the phenology of any particular crop type. This mixed pixel effect complicates the tracking of crop phenological progress and the characterization of phenological transition dates (Diao and Wang, 2016b; Peng et al., 2017). Hence, only the pixels with the fractions of corn or soybean greater than 90% in each agricultural statistics district were selected for constructing the pheno-network model and conducting the subsequent phenological analysis.

To date, the best available field-based crop progress and condition information at regional to state scales are Crop Progress Reports (CPRs), released by NASS, USDA. The CPRs record the percentage of major crops achieving a specific phenological development stage (e.g., mature stage of corn or dropping leaves stage of soybean), and are updated weekly by state NASS offices during the growing season from early April to late November (reports are available at https://www.nass.usda.gov/). Weekly CPRs are among the most popular and requested reports published by NASS, and have significant impacts on farming practices and agricultural market prices (Lehecka, 2014). About 4000 trained reporters across states conduct ground-level field observations of crop progress by following NASS standard definitions. These ground survey observations are aggregated and summarized to the ASD- or state-level to be reported in CPRs. ASD- or state-level reports provide a general summary of crop phenological development across multiple counties, and will serve as the ground reference data to evaluate the remotely sensed phenological retrieval results from the pheno-network model.

3. Methods

3.1. Pheno-network model

The pheno-network model is a newly developed framework for representing the time series of a pixel using complex networks. In the pheno-network model, the spectral reflectance obtained on each date of the time series is considered as a node, namely a spectral node. These nodes are further connected together according to their relationships, referred to as edges. The collection of nodes and edges constitutes a pheno-network. By formalizing the edges in different ways, the pheno-network model can be utilized to represent different behaviors of the satellite time series.

As the study focuses on estimating the critical phenological transition dates of crops in a satellite time series, two criteria are designed to construct the pheno-network. First, the edges are formalized according to the spectral similarity between the spectral nodes. The similarity between a pair of spectral nodes A and B is measured as the cosine distance between them:

$$\text{Distance}\ (A, B) = \cos^{-1}\left(\frac{A \cdot B}{||A||||B||}\right) \quad (1)$$

Here, A and B are vectors representing spectral reflectance of the nodes, and $Distance(A,B)$ is the cosine distance between A and B. $||A||$ and $||B||$ are the norms of the vectors A and B, respectively. A short cosine distance implies that the two nodes share similar spectral

reflectance. The cosine distance compares the similarity between the orientations of the vectors of spectral reflectance. It does not take into account the magnitudes of the vectors, and hence diminishes the influence of illumination and albedo differences on spectral reflectance.

Second, a "tolerance value" (d_0) is employed as a constraint to filter out connections between spectral nodes that share little similarity. In this way, the pheno-network only retains the edges with a cosine distance lower than the tolerance value. The tolerance value serves as a control parameter to adjust the level of temporal constraint embedded in the pheno-network model. As the change of crop phenology is a gradual process, the spectral nodes obtained on nearby dates are more likely to share similar spectral reflectance with shorter cosine distances. The spectral nodes at different phenological stages tend to be more distinct with longer cosine distances. With a sufficiently high tolerance value, the resulting pheno-network will become a fully connected network, meaning that every pair of spectral nodes are directly connected by edges. There is no temporal constraint on such pheno-network. In contrast, selecting a low tolerance value is equivalent to setting a strict temporal constraint on the pheno-network. This will result in a sparse network, where only spectral nodes representing nearby dates are directly connected. With different tolerance values, the pheno-network can model different temporal dynamic processes of crop phenology. Unlike conventional curve-fitting based phenological methods, where the time constraint is explicit, the pheno-network model implicitly embeds the time constraint into the tolerance value. That gives the model more flexibility to track various levels of crop phenological dynamics, as well as higher tolerances to missing and abnormal data in the satellite time series.

The pheno-network model typically needs to explore a range of tolerance values in order to identify the most appropriate one for estimating the phenological transition dates of crops. First, the candidate edges between all possible pairs of spectral nodes are created and sorted based on their cosine distances. Second, we locate the 5th, 10th, 15th, …, 95th percentiles of the sorted candidate edges, and select the corresponding cosine distances as the tolerance values. For example, when d_0 is set to the 5th percentile, the 5% of candidate edges with the smallest cosine distances are selected to construct the pheno-network. Each tolerance value will yield a single pheno-network. Network measures are calculated for each network to estimate the transition dates. The results are then compared between different networks to determine the most appropriate date.

3.2. Network measures of crop phenological transition dates

To detect the phenological transition period of crops, the pheno-network model needs to capture the spectral nodes that can represent the transition period using their network characteristics. The spectral reflectance of crops usually changes gradually before and after the phenological transition period, and dramatically during the transition period. In the network representation, those spectral nodes representing the dates before the transition period share comparable spectral reflectance and are inclined to form a densely linked group among themselves, referred to as the "pre-transition group". Similarly, those spectral nodes corresponding to the dates after the transition period would tend to form the "post-transition group". Due to the drastic change in spectral reflectance during the transition period, the two groups would have entirely different spectral reflectance and appear to be far apart in the network with few direct connections. Those spectral nodes representing the dates during the transition period would be linked to both the pre- and post-transition groups, and serve as a bridge standing between them. We refer those nodes as the "transition group". Among the three groups, the edges would be dense within the pre- and post-transition groups, as the change of spectral reflectance is gradual within these two periods, but sparse within the transition group because of the drastic change of spectral reflectance during this period. An example of a pheno-network with these three node groups is shown in Fig. 2.

As a whole, the transition group would consist of spectral nodes that serve as the hub connecting the nodes across all three crop phenological stages in the pheno-network. These nodes are also connected by relatively sparse edges between them. By virtue of the unique network-based representation, an innovative network measure, called "bridging coefficient", is designed in the pheno-network model to identify spectral nodes possessing these characteristics. For a node i, its bridging coefficient, noted as bc_i, is the ratio of its betweenness centrality and clustering coefficient:

$$bc_i = \frac{b_i}{c_i} \tag{2}$$

Here, b_i and c_i are the betweenness centrality and clustering coefficient values of node i, respectively. Some pairs of nodes in a network are directly connected by an edge, while others need to be linked by a chain of edges, called "paths". In path-based connections, there may be multiple paths connecting a pair of nodes, and each of the paths may comprise different number of edges. Among these paths, the one with the lowest number of edges is taken as the shortest path between the pair of nodes. The betweenness centrality of node i is calculated as the fraction of all shortest paths between all pairs of nodes that pass through node i (Freeman, 1978):

$$b_i = \sum_{s \neq t \neq i} \frac{\sigma_{st}(i)}{\sigma_{st}} \tag{3}$$

Here, σ_{st} is the total number of shortest paths between a pair of nodes s and t, and $\sigma_{st}(i)$ is the number of these paths that go through node i. A node with a high betweenness centrality value has a large fraction of shortest paths passing through it and plays an important role in linking other nodes together in the network. For example, a network of airports consists of all airports as nodes and flights between airports as edges. The O'Hare international airport in Chicago, IL is one of the nodes with high betweenness centrality values, as it serves as a regional hub for a large number of airports in the Midwestern United States (Jia et al., 2014). As for the pheno-network case, all paths connecting the pre- and post-transition groups need to pass through the spectral nodes in the transition group. These nodes would have high betweenness centrality values in the network representation. Despite the importance of betweenness centrality in identifying the nodes in the transition group, we find that the irregular or abnormal spectral nodes, caused by atmospheric interference and noise, might have comparable betweenness centrality values. To reduce the effects of those spectral nodes, another network measure, namely clustering coefficient, is taken into account.

The clustering coefficient of a node is measured as the total number of edges between its neighbors divided by the maximum number of edges that potentially exist between the neighbors (Watts and Strogatz, 1998):

$$c_i = \frac{2|\{e_{jk}\}|}{k_i(k_i - 1)} \tag{4}$$

Here, nodes j and k are any two neighbors of node i, and e_{jk} is the edge between these two nodes, and k_i is the total number of neighbors of node i. The clustering coefficient measures the extent to which neighbors of a node cluster together, and tends to be low for the nodes with sparse edges in the pheno-network. Due to the rapid change of spectral reflectance during the transition period, the neighbors of the nodes in the transition group are inclined to be sparsely connected to each other. As discussed above, the spectral nodes in the transition group would have high betweenness centrality and relatively low clustering coefficient values, which gives rise to high bridging coefficient values. With this network measure, the pheno-network model is to capture those spectral nodes that are characteristic of the crop phenological transition period.

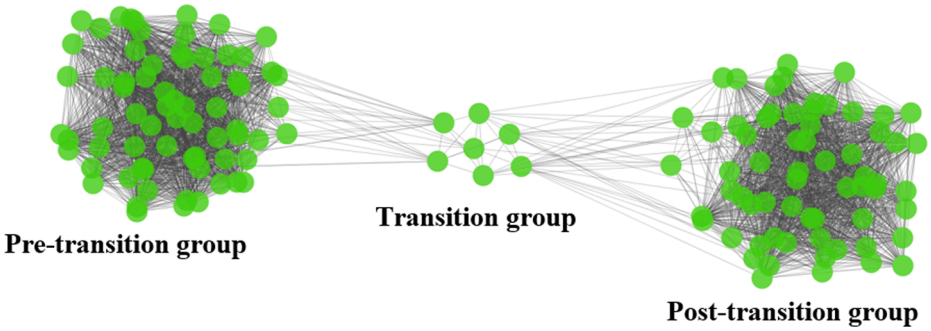

Fig. 2. Pheno-network with three groups, namely the pre-transition, transition, and post-transition groups.

The compositing process of the MCD43A4 data, along with its pre-processing via quality assurance layers, is utilized to filter out the abnormal and outlying spectral reflectance in this study. To further reduce the influence of potential abnormal (or outlying) spectral nodes on the network-derived measures, a moving window is applied to calculate the average bridging coefficient for each observation date to smooth out fluctuations. For example, a seven-day moving window of an observation date includes its three preceding days and three succeeding days. After experimenting a range of moving window sizes (i.e., one to ten days), the seven-day moving window was found to be the best tradeoff among spectral smoothness, spectral representations of nodes, and duration of crop phenological transition periods. Hence, the average bridging coefficient within a seven-day moving window of each observation day is calculated as its moving average bridging coefficient. Since there is no clear boundary of the crop phenological transition period, we focus on estimating the most critical phenological transition date, namely the date with the highest moving average bridging coefficient value.

As discussed in Section 3.1, this study explores a range of tolerance values, each of which yields a unique pheno-network (Fig. 3). For a given network, the moving average bridging coefficient will be calculated for all spectral nodes. The spectral node with the highest value and the corresponding date will be identified. We will then compare all identified nodes among all pheno-networks and select the spectral node with the highest moving average bridging coefficient as the critical crop phenological transition date.

3.3. Accuracy assessment

With the moving average bridging coefficient measure of the pheno-network model, the phenological transition dates for the downward period of a pixel can be estimated. For all the corn and soybean pixels considered in Illinois, the transition dates are calculated through the pheno-network model for all the monitoring years (2002–2017). The retrieved phenological transition dates are compared to the field-based observations of crop phenological progress in CPRs at ASD levels. For each ASD, the cumulative percentages of the retrieved transition dates over time are calculated for both corn and soybean. The derived cumulative percentages are then compared to the percentage of crops going into specific phenological development stages in CPRs. For instance, the cumulative percentage of the retrieved transition dates of corn during the downward period is compared to the percentage of corn entering the dough, dent, mature, and harvest stages, respectively. The comparisons are expected to unveil how pheno-network retrieved phenology aligns with field-based phenological observations. For the crop phenological stage most closely relevant to the pheno-network retrieved result, the median date of crop achieving that stage is compared to that of the corresponding transition dates using root mean square error (RMSE) and R square.

The performance of the pheno-network model is further compared to that of a parametric curve-fitting based phenological method. As one

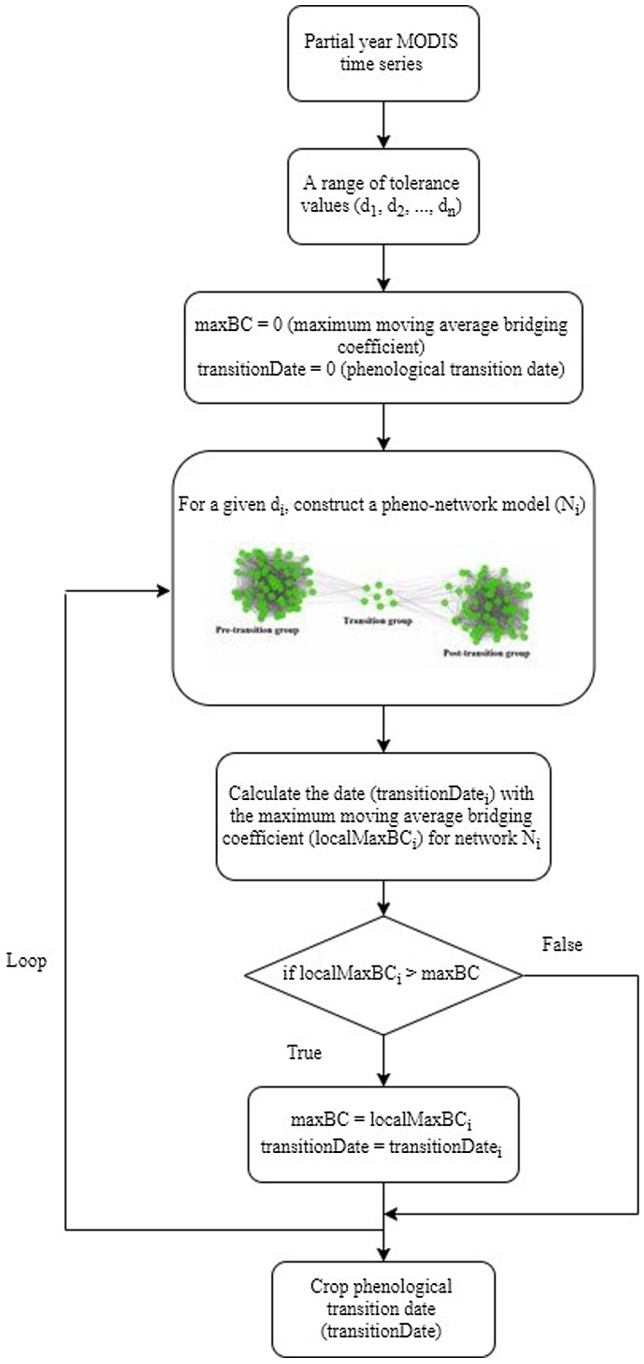

Fig. 3. Diagram of the methodology.

of the most widely used phenological curve-fitting methods, the double logistic method is utilized in this study to retrieve the phenological transition dates of crops using year-long satellite observations (Zhang et al., 2003). It assumes that the phenological trajectory of crop development can be modeled using the logistic functions, and fits the logistic curve to the NDVI observations over the course of a year. The rate of change in the curvature of the fitted curve is then employed to retrieve the crop phenological transition dates. It estimates the transition dates by capturing the local extremes (e.g., minimum or maximum) in the rate of change in the curve curvature. For all the corn and soybean pixels in Illinois throughout 2002–2017, the transition dates of the onset of dormancy are calculated using the curve-fitting based method, and compared to those from the pheno-network model using the ground reference data.

The conventional curve-fitting based phenological methods typically require year-long satellite observations to estimate the phenological transition dates. In contrast, the pheno-network model can be constructed with partial-year remote sensing data (e.g., pheno-network model for the downward period). The size of the temporal window defines the maximum number of spectral nodes considered in the model. In this study, the role of the size of the temporal window in estimating phenological transition dates is evaluated through sensitivity analysis. Specifically, a multitude of temporal segment windows for the downward period of corn and soybean are tested for phenological estimates. The size of temporal segment windows for constructing the pheno-network model varies from 140 days (day of year [DOY] 191–330) to 20 days (DOY 251–270), with an increment of 10 days. Each time the change of the temporal window size is via 5 days deduction from both ends of the window, with reference to field-observed crop phenological progress. For example, when the size of the temporal window reduces from 140 days to 130 days, the window changes from DOY 191–330 to DOY 196–325. This way in changing the temporal window size would ensure that the critical phenological transition periods could be included in most of testing windows. For each temporal segment window, the median date of the estimated transition dates is compared to that of the corresponding field-observed phenological stage using RMSE and R square.

4. Results

By defining the nodes of spectral reflectance and edges of spectral similarities between the nodes, the pheno-network model characterizes the structure of temporal dynamics of remotely sensed spectral reflectance along the phenological trajectory. It provides a network-based representation of the crop phenological process. In this study, the pheno-network model was constructed for each corn or soybean pixel of Illinois during the downward period of a year. With a corn pixel in 2006 as an example, the network representation of its downward phenological progress was shown in Fig. 4a. Three node groups, namely the pre-transition, transition, and post-transition groups, could be roughly identified in this pheno-network. The colors of the nodes denoted the values of the moving average bridging coefficients, with an orange tone indicating a high moving average value, a yellow tone denoting a value in the middle, and a blue tone suggesting a low value. Compared to the ones in pre- and post-transition groups, the spectral nodes in the transition group had higher moving average bridging coefficient values. In Fig. 4a, the nodes in the transition group served as the bridging hub connecting the nodes across groups, and exerted a critical role in controlling the temporal phenological dynamics of spectral reflectance. The neighbors of those nodes were sparsely connected between themselves. Through integrating the betweenness centrality and clustering coefficient, the bridging coefficient measure was characteristic of the distinct network structure during the transition period of crop phenology. The high moving average bridging coefficient values of those transition nodes indicated that this network measure could be utilized to capture the node representing the critical phenological transition date of crops.

During the downward period (DOY 191–330) of the pixel, the one-day bridging coefficient (i.e., without moving average) and seven-day moving average bridging coefficient of each observation date were shown in Fig. 4b. Compared to the one-day network measure, the moving average bridging coefficient exhibited much smoother and clearer temporal patterns of spectral nodes. Specifically, the spectral nodes around DOY 255–265 achieved high moving average bridging coefficient values, with the highest one at DOY 260 representing the critical phenological transition date. These nodes were colored in orange in the pheno-network, demonstrating their transitional roles in representing the crop phenological progress (Fig. 4a). The fluctuations of the one-day bridging coefficient values, including relatively high values at DOY 241 and 272, were smoothed out in the seven-day measures. Thus the moving average bridging coefficient could further reduce the outlying and abnormal spectral reflectance in the satellite time series caused by atmospheric interferences.

With the pheno-network model, the phenological transition dates during the downward period were estimated for all relatively pure corn and soybean pixels in Illinois. The cumulative percentages of the transition dates were calculated and summarized according to ASDs from 2002 to 2017. For corn, this cumulative percentage of the transition dates was compared to the ground reference cumulative percentage of corn going through the dough, dent, mature, and harvest stages, respectively (Fig. 5, with 2006 as an example). In light of the ground survey data, corn entering the dough stage varied from location to location in 2006, with the earliest around DOY 183 and the latest around DOY 239. Across the ASDs, the median date of the dough stage of corn in the southern districts was around 8 days earlier than that of

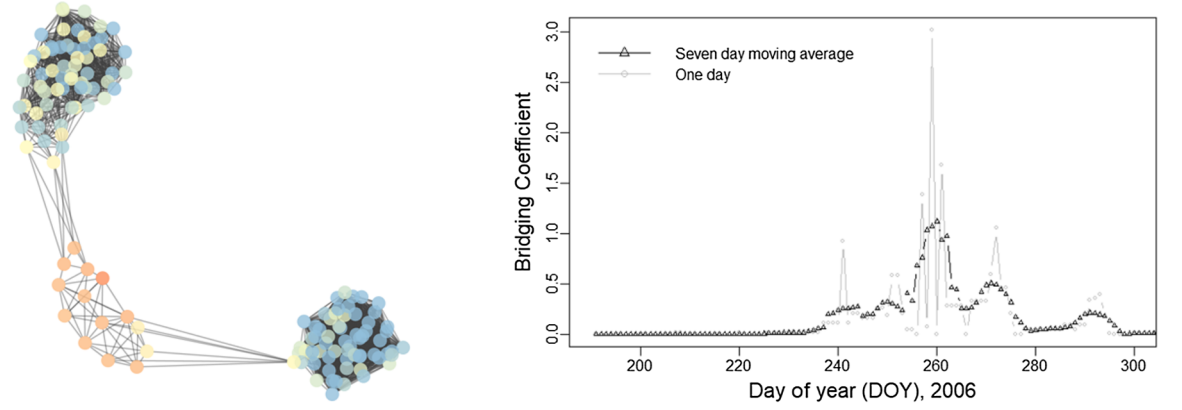

(a) Pheno-network of a corn pixel in 2006 (b) Network measures of spectral nodes in the pheno-network

Fig. 4. Network measures of crop phenology to estimate the critical phenological transition date.

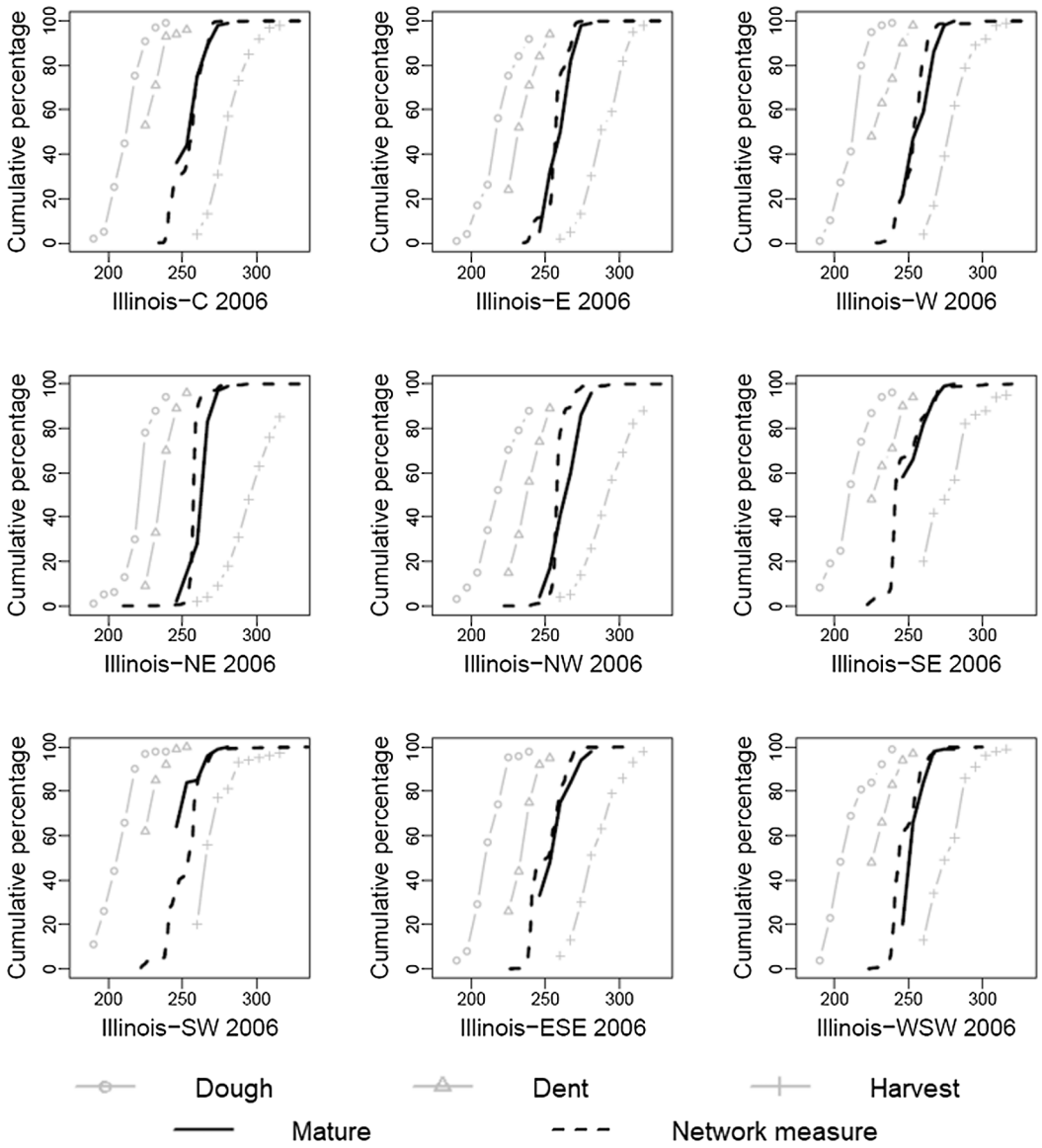

Fig. 5. Comparisons between the cumulative percentage of the transition dates and ground reference cumulative percentages of corn going into the dough, dent, mature, and harvest stages in 2006 at the district level.

the central districts, which was on average 7 days before that in the northern districts. Following the dough stage, corn went into the dent stage from DOY 225 to 253, then to the mature stage from DOY 246 to 281, and finally to the harvest stage from DOY 260 to 316. The cumulative percentage of the transition dates estimated through the pheno-network model ranged from DOY 241 to 276, and was found to align well with that of the mature stage of corn (Fig. 5). In 2006, the median ground observation date of corn entering the mature stage throughout Illinois was DOY 256, which was the same as the median transition date (i.e., DOY 256) estimated using the pheno-network model.

The cumulative percentage of the retrieved phenological transition dates was also calculated for soybean, which was compared to the ground reference cumulative percentage of soybean entering the setting pods, turning yellow, dropping leaves, and harvest stages, respectively (Fig. 6, with 2006 as an example). According to the ground reference data, soybean started to set pods during the reproductive stages from DOY 190 to 239 throughout Illinois. Following the setting pods stage, the leaves of soybean turned yellow around DOY 246 to 267, and typically started to drop one week after. Similar to corn, soybean also exhibited spatial variation in phenological development across agricultural districts. Affected by a combination of climate factors and management strategies, the median date of the dropping leaves stage of soybean in the southern districts was about one week behind that in the central and northern districts. Subsequently, the soybean was harvested, with the date varying from DOY 274 to 316. The cumulative percentage of the derived transition dates was compared to those four phenological development stages of soybean, and was found to be more correlated with that of the dropping leaves stage of soybean (Fig. 6). Throughout Illinois, the median date of soybean (i.e., DOY 264) going into this phenological stage in terms of ground observations was one day different from that of the pheno-network derived estimate (i.e., DOY 263) in 2006.

The retrieved phenological transition dates from the pheno-network model were summarized for both corn and soybean at the state level from 2002 to 2017 (Figs. 7 and 8). As regards corn, the cumulative percentage of the transition dates over time was shown as the dashed line, and the cumulative percentage of corn achieving the mature phenological stage was depicted as the solid line in Fig. 7. In most of the monitoring years, the phenological pattern of the ground-observed mature stage throughout Illinois could be approximated by that of pheno-network derived measures. These two cumulative curves aligned

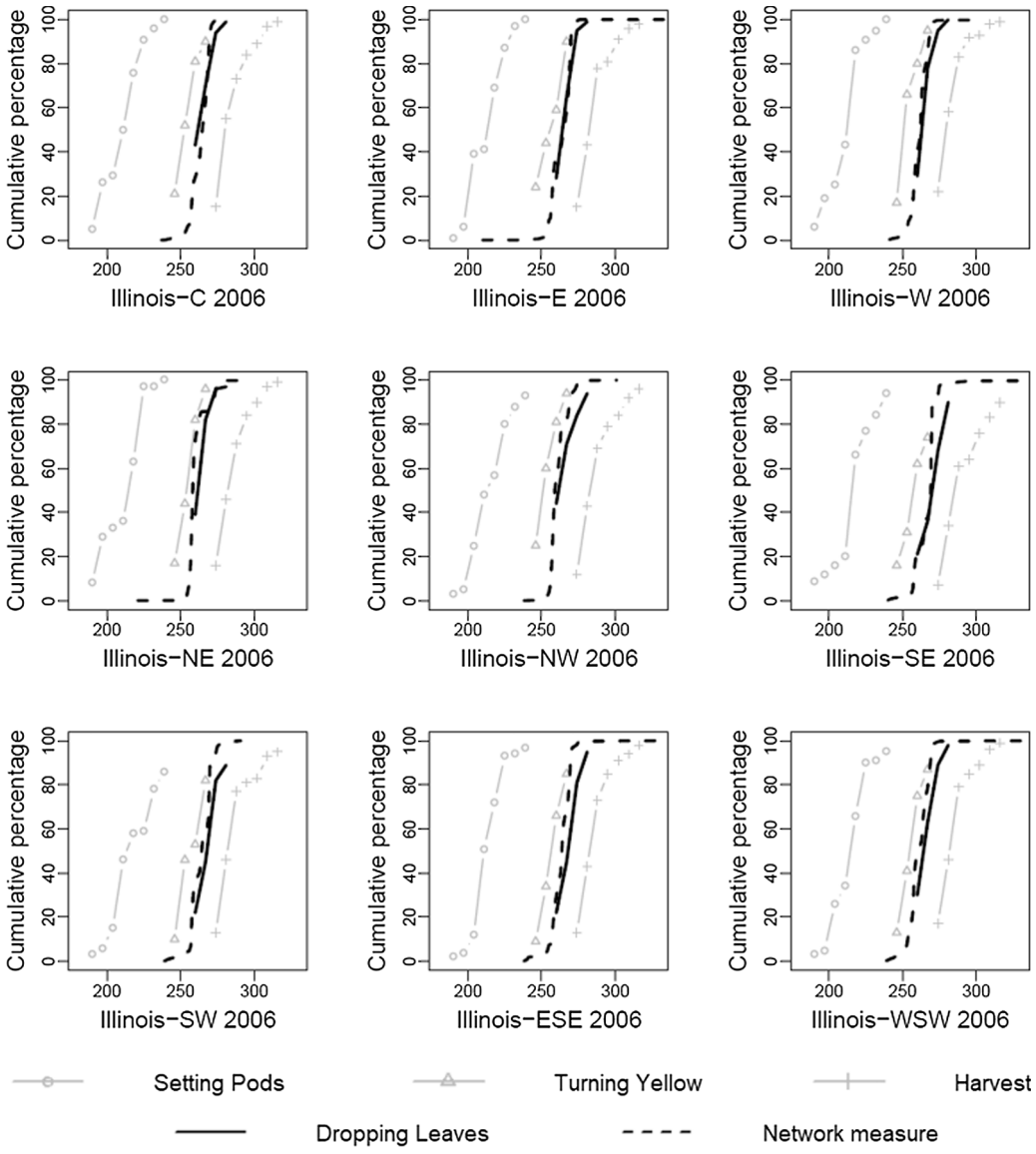

Fig. 6. Comparisons between the cumulative percentage of the transition dates and ground reference cumulative percentages of soybean entering the setting pods, turning yellow, dropping leaves and harvest stages in 2006 at the district level.

with each other well. Due to the weekly observation interval for ground crop phenology and the missing data issue in CPRs, we further evaluated the alignment by focusing on calculating the difference between the median date of corn in the mature stage and the median of the estimated transition dates (Table 1). During 2002 to 2017, the absolute difference of median dates varied from 0 to 10 days, with an average of 4.5 days. These comparisons indicated that the retrieved phenological transition date was characteristic of the mature stage of corn. At this phenological stage, corn is about ready to harvest with shucks opening. The foliage of corn turns yellow, with no green color tone remaining. The spectral reflectance of corn is different from that in the preceding growth stages (e.g., dough and dent stages) and from that in the succeeding stages (e.g., harvest). It serves as the transition from green leaf-dominating spectral reflectance to soil-dominating harvest reflectance.

The moving average bridging coefficient was calculated for each spectral node in the pheno-network. The phenological transition date, identified by the maximum moving average bridging coefficient value, indicated that the spectral node on that date was a connecting hub linking all the spectral reflectance across the crop growth stages. As the bridging coefficient was a synthesized measure of betweenness centrality and clustering coefficient, the neighbors of the identified spectral node tended to be loosely connected between themselves because of the rapid change of spectral reflectance during the transition period. The spectral node at the phenological transition date had significant controls on the spectral dynamic changes along the crop leaf senescence trajectory. Characterized by a combination of changing leaf color, leaf water content, and leaf cell structure, the nodes at the mature stage of corn in the pheno-network are spectrally distinct, yet serve as the transitional bridge connecting the nodes from the leaf-on dough (or dent) stage to the leaf-off harvest stage. The unique network structure formulated according to spectral similarities is characteristic of the complex phenological process, and the network measures can be employed to estimate transition dates with critical phenological implications. This mature stage of corn has not been adequately captured in previous remotely sensed phenological studies (but see Sakamoto (2018) for phenological estimates with prior information), yet can be represented by the pheno-network model.

The phenological transition dates of soybean retrieved by the pheno-network model at the state level were summarized in Fig. 8. From 2002 to 2017, the cumulative percentage of remotely sensed transition dates throughout Illinois was compared to that of soybean going into the dropping leaves phenological stage on ground. As shown

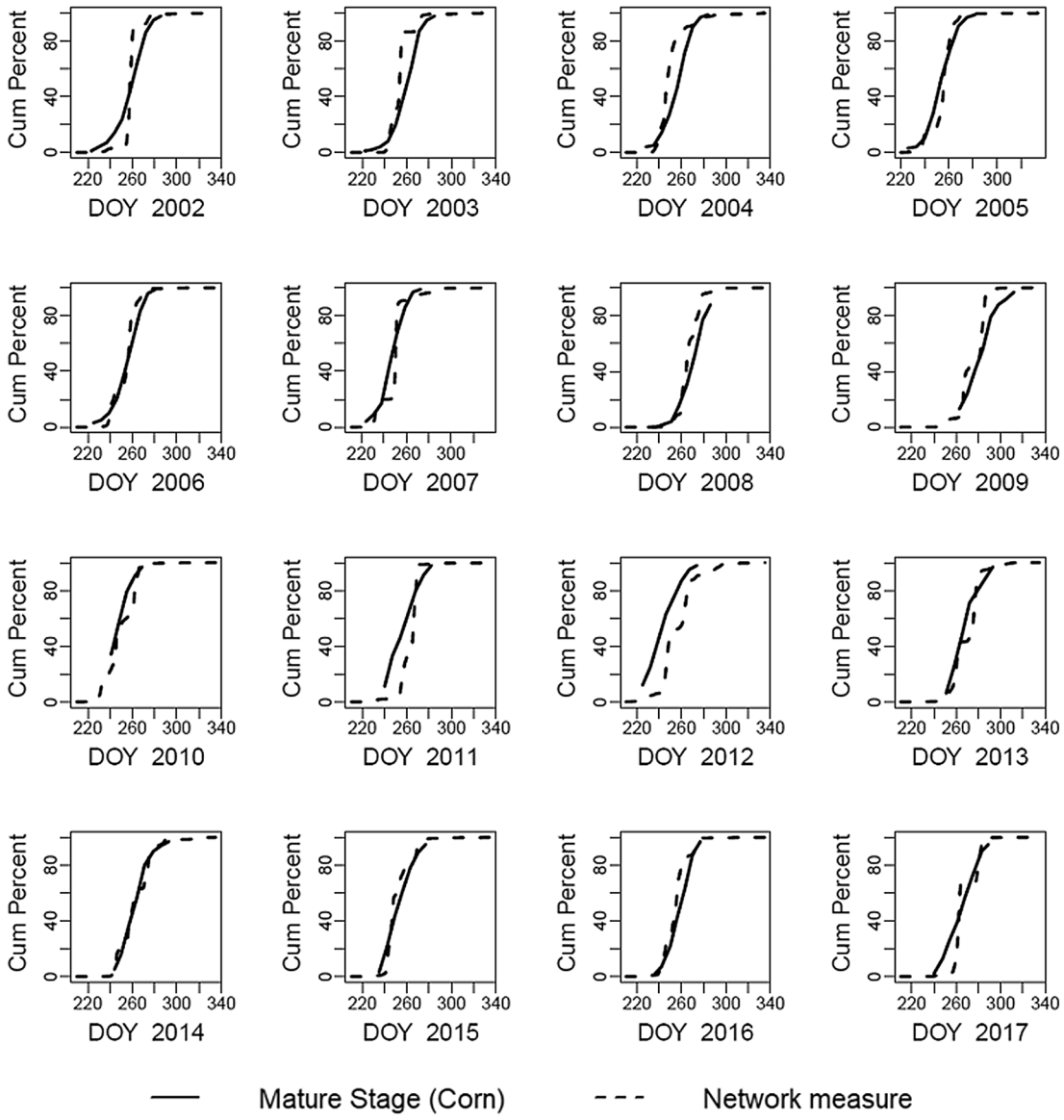

Fig. 7. Comparisons between the cumulative percentage of the transition dates and the ground reference cumulative percentages of corn going into the mature stage at the state level from 2002 to 2017.

in Fig. 8, this remotely sensed cumulative estimation result aligned well with the ground-based phenological observations in most years. The phenological pattern of the dropping leaves stage of soybean throughout Illinois was closely correlated with that of the pheno-network retrieved measures. The median of the estimated transition dates ranged from DOY 251 to 275 across the years (Table 1). Comparably, the median date of soybean entering the dropping leaves stage from CPRs varied from DOY 256 to 273. The absolute difference of median dates varied from 1 to 10 days, with an average of 4.4 days. The comparisons revealed that the dropping leaves phenological stage of soybean could be remotely retrieved by the pheno-network model with satellite time series. At this growing stage, the leaves of soybean are 30–50% yellow and the leaves near the bottom part start dropping. Similar to the mature stage of corn, the spectral reflectance of soybean at the dropping leaves stage (e.g., leaves changing to a yellowish tone with decreasing water content) exerts a critical transitional role in connecting the spectral reflectance across the phenological stages in the pheno-network. It serves as the transitional bridge from the green leaf-dominating growth stages (e.g., setting pods and turning yellow) to the soil-dominating harvest phenological stage. Therefore, the temporal dynamic changes of spectral reflectance of both corn and soybean along the phenological trajectory can be represented via network structures. The critical phenological transition dates can then be estimated through the corresponding network measures.

To further evaluate how remotely retrieved phenological transition dates reconcile with ground-based phenological observations, the median dates retrieved by the pheno-network model and by the curve-fitting based method were compared at the ASD level using R square and RMSE (Fig. 9). For each ASD, the median of pheno-network retrieved (or curve-fitting retrieved) transition dates for every year (horizontal axis in Fig. 9) was plotted against the median date of crop achieving the most relevant growth stage, namely the mature stage of corn or dropping leaves stage of soybean (vertical axis in Fig. 9). The one-to-one line in Fig. 9 denoted that remotely retrieved and ground observed median measures matched each other exactly. As for corn, most of these comparison pairs by the pheno-network model were distributed along the one-to-one line, with the R square being 0.55 and the RMSE being 7.77 days. It indicated that about 55% percent of variability in the median dates of ground-observed mature stage of corn could be explained by the pheno-network based measures. The average

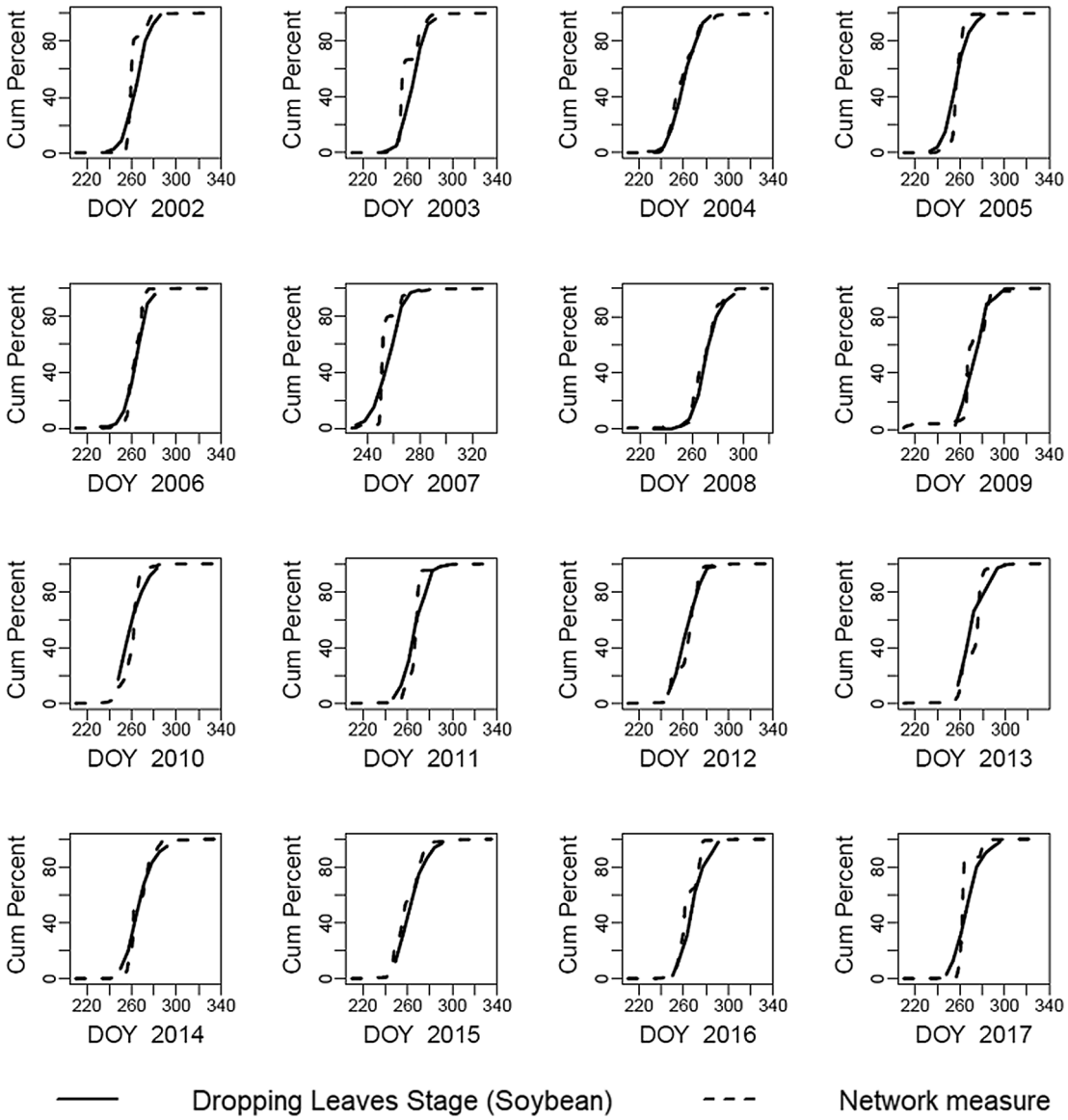

Fig. 8. Comparisons between the cumulative percentage of the transition dates and the ground reference cumulative percentage of soybean entering the dropping leaves stage at the state level from 2002 to 2017.

of the difference between the network- and ground-based maturity measures was around 7 days. Given the weekly observation frequency of CPRs and the compositing process in the daily 16-day MODIS data, the 7-day difference should be adequate for demonstrating the capabilities of the devised pheno-network model in retrieving critical crop growth transition dates, particularly for large-scale repetitive estimation. As for the curve-fitting based method, most of these comparison pairs were distributed below the one-to-one line, with the R square being 0.56 and the RMSE being 26.8 days. It indicated that the median transition dates estimated by the curve-fitting method were about 3–4 weeks later than the median dates of ground-observed mature stage of corn. Thus this critical phenological stage of corn might not be appropriately represented by the curve-fitting retrieved phenological measures.

As regards soybean, the comparison pairs by the pheno-network model at the ASD level were also distributed along the one-to-one line (Fig. 9). The R square value was 0.55 and the RMSE value was 5.05 days. About 55% percent of variability in the median dates of field-based dropping leaves stage of soybean was explained by the median of estimated transition dates. The average of the difference between the network- and ground-based phenological measures was about 5 days. In Fig. 9, the comparison pairs for soybean were mostly distributed within the temporal window DOY 250 to 280 across ASDs throughout the years, while the comparison pairs for corn were distributed in a wider temporal range DOY 230 to 285. It indicated that, compared to the dropping leaves stage of soybean, there was higher spatial and inter-annual variability in the mature stage of corn throughout Illinois. Though the further comparative analysis was beyond the scope of this study, the comparable and relatively high R square values suggested that the spatio-temporal variability in the ground phenological observations could be captured by the pheno-network derived measures. With respect to the curve-fitting based method, most of the comparison pairs were below the one-to-one line, with the R square being 0.5 and the RMSE being 22.36 days. Comparable to corn, the median transition dates estimated by the curve-fitting method were noticeably later than the median dates of ground-observed dropping leaves stage of soybean. The curve-fitting derived phenological measures of soybean were about 2–3 weeks after its dropping leaves stage.

As the turning yellow stage and dropping leaves stage of soybean were closely related and typically one week apart (e.g., Fig. 6), we

Table 1
Comparisons between the median of pheno-network retrieved transition dates and the median date of corn in the mature stage (left), or soybean in the dropping leaves stage (right) at the state level from 2002 to 2017.

Year	Corn (mature stage)		Soybean (dropping leaves stage)	
	Ground reference (DOY)	Pheno-network estimated (DOY)	Ground reference (DOY)	Pheno-network estimated (DOY)
2002	260	258	265	259
2003	260	253	265	255
2004	257	247	260	257
2005	253	256	256	257
2006	256	256	264	263
2007	247	250	256	251
2008	271	265	271	269
2009	281	281	273	267
2010	246	246	257	262
2011	256	266	265	267
2012	241	251	262	265
2013	266	274	268	275
2014	262	260	266	262
2015	252	247	262	257
2016	259	255	267	261
2017	265	263	266	262

further evaluated the alignment between the median date of soybean going into the turning yellow stage and that of the pheno-network estimated transition dates (Fig. 10). As shown in Fig. 10, the comparison pairs shifted away from the one-to-one line, with the RMSE value increasing to 10.59 days and R square value decreasing to 0.47. Despite the amount of variability in this turning yellow stage explained by the pheno-network measures, the increasing difference between these two measures and the deviation from the one-to-one line suggested that the estimated transition dates might not be directly indicative of the turning yellow stage of soybean. In general, these quantitative measures conducted at the ASD level implied that the transition dates estimated by the pheno-network model had remarkable phenological implications. The critical phenological stages (i.e., the mature stage of corn and the dropping leaves stage of soybean), which may not be adequately captured with conventional phenological models, can be retrieved via innovative network structures.

One significant challenge in conventional phenological models is the requirement of year-long satellite observations for model building. In contrast, the pheno-network model can be constructed with partial-year remote sensing data. A sensitivity analysis was conducted in this study to evaluate the influence of the temporal window size on the retrieved phenological transition dates. With reference to field crop phenological stages, the size of the temporal window for constructing the pheno-network model changed from 140 days (DOY 191–330) to 20 days (DOY 251–270), with an increment of 10 days. With respect to each temporal window, the median date of the estimated transition dates was compared to that of the corresponding ground-observed phenological stage at the ASD level using R square and RMSE (Fig. 11).

With the increasing size of the temporal window, the R square value for corn rose from 0.15 to 0.61 and the RMSE value decreased from about 10 to 7 days. When the size of the temporal window increased to 80 days, the R square value achieved 0.5, along with the RMSE value decreasing to around 8 days. Hence, the pheno-network model showed great potential in estimating the mature stage of corn within a limited temporal observation period. Compared to corn, the R square and RMSE values of soybean changed even more drastically with the increment of the temporal window size. The R square value approached 0.5 and the RMSE value decreased to around 5.5 days with a temporal window size of 40 days. This more rapid increase of R square values and decrease of RMSE values may be attributable to two factors. First, soybean typically has a shorter growing season than corn. The transition date for soybean is more inclined to be identified than that for corn given a limited temporal window. Second, the dropping leaves stage of soybean exhibits lower spatial and inter-annual variability across ASDs, compared to the mature stage of corn (Fig. 9). The sensitivity analysis revealed that the pheno-network model could be built with partial-year satellite observations. The network structure for identifying the phenological transition dates was relatively robust to the change of the number of spectral nodes arising from the changing temporal window size.

5. Discussion

In recent years, complex networks have been increasingly utilized in a variety of disciplines, ranging from social science to biological science, to investigate the associations and relationships between the constituents of complex systems. The network representation is designed to capture the most fundamental structure and pattern of key components in a system. The flexibility of defining the nodes and edges in complex networks opens up unique opportunities to understand and characterize collective behaviors of inter-connected components in complex systems. This continuously flourishing network representation has nurtured breakthrough discoveries and insights in a wealth of fields, yet it has seldom been explored in time series remote sensing.

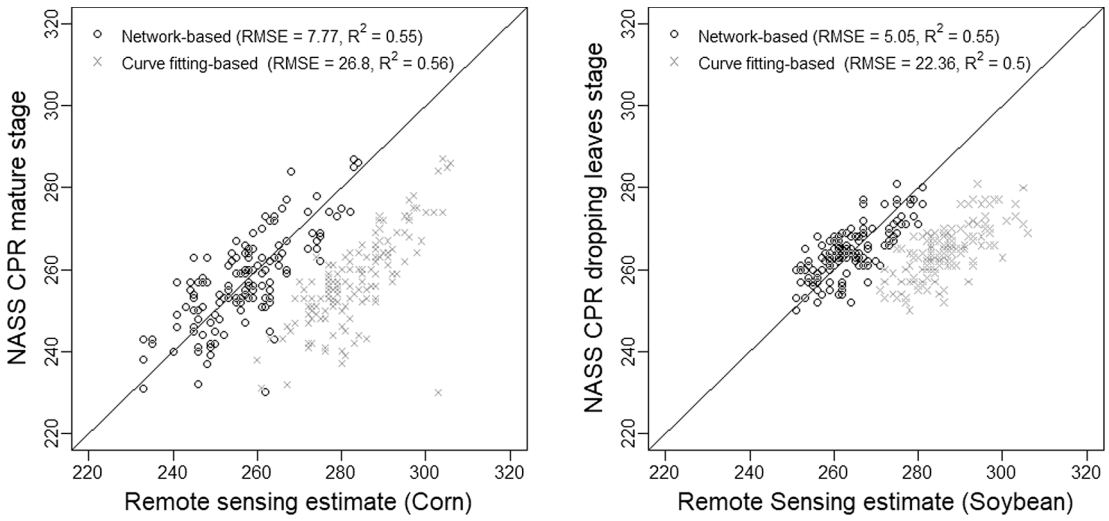

Fig. 9. Comparisons between the median of remote sensing retrieved transition dates and the median date of corn in the mature stage (left), or soybean in the dropping leaves stage (right) at the district level using R square and RMSE.

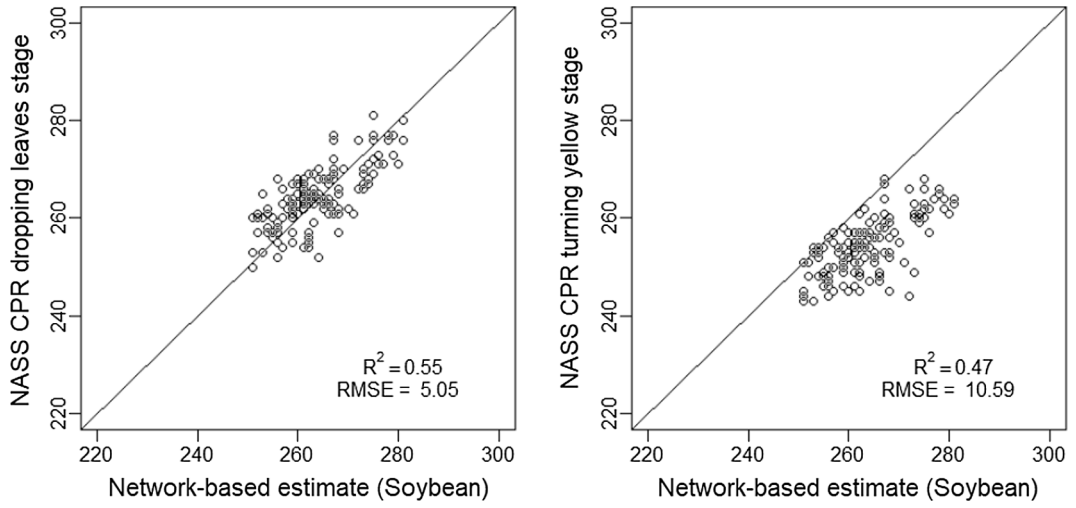

Fig. 10. Comparisons between the median of pheno-network retrieved transition dates and the median date of soybean in the dropping leaves stage (left), or the turning yellow stage (right) at the district level using R square and RMSE.

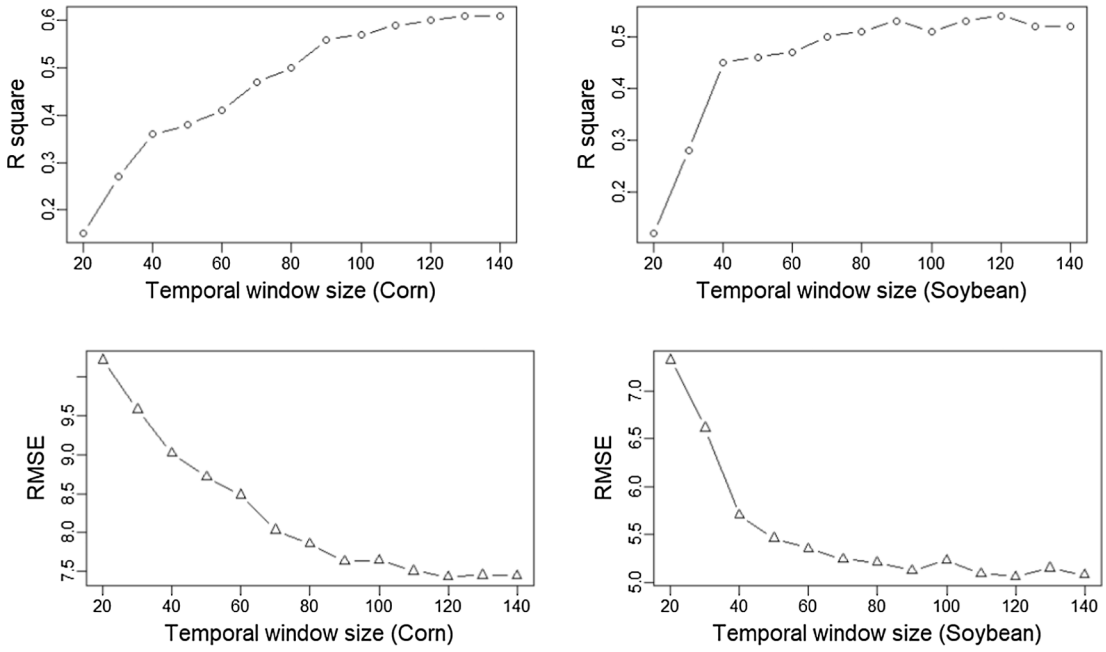

Fig. 11. The R square and RMSE values of the pheno-network retrieved results with varying temporal window sizes.

The potential of complex networks in representing the complex crop phenological progress with satellite time series was hence investigated in this study.

The pheno-network model provides an innovative phenological representation of crop through modeling the temporal dynamics of its spectral reflectance along the leaf senescence trajectory. This network representation characterizes the structure of relationships between the spectral reflectance to estimate the critical phenological transition dates. In the pheno-network, the nodes are defined as the spectral reflectance of crops on each observation date, and the edges are defined according to the spectral similarities between the nodes. The tolerance value controls the structure of the entire network. The moving average bridging coefficient is devised as the network measure to capture the spectral nodes that serve as the transitional bridge in linking the spectral reflectance across the phenological stages. By integrating betweenness centrality and clustering coefficient, this synthesized measure weights the neighborhood connection effects to identify the spectral nodes as the connecting hub in the network. This new phenological representation was able to estimate the crop phenological transition dates in Illinois, particularly the mature stage of corn and the dropping leaves stage of soybean, with high accuracy achieved. At the ASD level, the R square values for both corn and soybean are 0.55. The RMSE values for corn and soybean are 7.77 and 5.05 days, respectively. The pheno-network model shows marked potential to extract crucial crop phenological characteristics, complementary to the conventional phenological methods.

Compared to conventional curve-fitting based phenological methods, the pheno-network model maintains several distinct characteristics and potential advantages. First, the pheno-network model does not assume that crop phenological processes follow specific mathematical functions. Without limiting the phenological processes to defined mathematical forms, this non-parametric model may be more adequate to characterize the complex crop phenological trajectory, particularly in diversified and intensified agricultural systems. Second, the pheno-network model can be constructed with partial-year remote sensing data. Unlike the conventional curve-fitting based phenological

methods, the pheno-network does not require the year-long data for model building. The sensitivity analysis conducted in this study indicates that the pheno-network model can be built within a limited temporal observation period (e.g., 80 days for corn). The pheno-network model is relatively robust to the change of the temporal window size for estimating critical phenological transition dates. Third, the pheno-network model tracks the collective change of spectral reflectance for phenological estimation. Remotely sensed crop phenology is typically monitored using the time series of vegetation index (e.g., NDVI, enhanced vegetation index [EVI], and wide dynamic range vegetation index [WDRVI]). As vegetation indices are developed for characterizing specific vegetation properties, the adoption of different vegetation indices may yield different or even conflicting phenological estimation results (Tornos et al., 2015). Tracking the collective change of spectral reflectance along the phenological trajectory may be an alternative solution, given the vegetation properties (e.g., chlorophyll content, water content, and leaf cell structure) can be characterized by a multitude of spectral wavelengths. Therefore, with these unique characteristics, the pheno-network model provides an innovative perspective in representing the crop phenological process. In this study, the retrieved phenological estimates, in alignment with ground phenological observations, also indicate that the pheno-network model shows great promise in monitoring the crop growth progress and understanding its subsequent response to climate and environmental changes.

Along the leaf senescence trajectory, the estimated critical phenological transition periods via the pheno-network model are the mature stage for corn and the dropping leaves stage for soybean. Corn and soybean share comparable traits during their respectively detected stages. Their leaves change to yellowish tones, with drastic chlorophyll and water content change. Corn is about to harvest within 2–4 weeks and soybean is about to harvest within 2–3 weeks. Hence, accurate estimation of those phenophases are imperatively crucial for operational harvest preparation and scheduling to reduce pre-harvest loss. The crop growth conditions at those phenophases are important for crop management and yield estimation. Remotely sensed retrieval of crop growth stages may further shed light on the crop phenological responses to climate change and environmental stress, as well as the changing farm management practices and strategies (e.g., development of new crop genotypes) (Kucharik, 2006). Yet those critical phenophases have not been adequately captured by previous studies. With the curve-fitting (i.e. double logistic) based phenological method, Gao et al. (2017) retrieved the dormancy dates for both corn and soybean in central Iowa using satellite time series. The dormancy date retrieved for corn was found to be between its mature and harvest stages. The retrieved dormancy date for soybean was between the dropping leaves and harvest stages. Given the phenological implications of those growing stages, it would be desired to have more accurate retrieval results from remote sensing.

Validating the remotely sensed phenology with ground-based observations remains one of the most significant challenges in phenological studies. The ground-based phenological measure of individual crop may not match with that of 500 m spatial coverage of an individual pixel in the MODIS imagery. Besides, the field observation locations of crop phenology are proprietary and not available to the public in CPRs. Only the aggregated phenological observations at the ASD- or state-levels are released by NASS. At the ASD level, the good alignment between ground-based and remotely sensed crop phenology in this study demonstrates the potential of the proposed pheno-network model in estimating critical crop phenological transition dates. Despite being the most comprehensive dataset throughout Illinois, the ASD- or state-level phenological aggregates and the CDL-based MODIS aggregates may bring some uncertainties to the evaluation results. The recent initiative in near-surface remote sensing (e.g., unmanned aerial vehicle and phenocam) may provide solutions to collect geo-referenced ground phenological observations of crops in a more systematic and objective fashion, which may facilitate the pixel-based phenological evaluation and reduce the uncertainties arising from the ASD-level comparisons (Richardson et al., 2018). It would be conducive to explore those near-surface remote sensing techniques in future studies.

Remote monitoring of crop phenological progress at 500 m spatial resolution benefits the large-scale crop management and yield estimation. The pixel-based phenological estimates, beyond the ASD-level, provide farmers substantial information at finer spatial granularity to advance crop and farm management strategies that can ultimately alleviate environmental stresses in crops and improve crop productivity (Wu et al., 2013; Zhou et al., 2017). With its daily 16-day compositing and BRDF-corrected properties, the MCD43A4 data is a desired candidate for conducting the repetitive phenological monitoring over wide geographical regions through time. Despite its high temporal revisit frequency, its coarse spatial resolution (i.e., 500 m) may make it inadequate for capturing field-level crop phenological dynamics, particularly in smallholder agricultural systems. Under those circumstances, it may be conducive to build the satellite time series by synthesizing the higher spatial resolution imagery (e.g., Landsat and Sentinel-2) with the MODIS imagery using data fusion algorithms (Feng et al., 2006). With both higher spatial and temporal resolutions (e.g., daily imagery at 30 m spatial resolution), the fused imagery may help retrieve more comprehensive phenological information to further benefit the smallholder agricultural systems.

6. Conclusions

In this study, we estimated the critical phenological transition dates of crops via an innovative pheno-network model. Rooted in network theory, this model characterizes the complex phenological process with spectrally defined nodes and edges. It provides a network representation to model the temporal dynamics of spectral reflectance of crops along the phenological trajectory. With the moving average bridging coefficient measure, the pheno-network model attempts to capture the spectral nodes that serve as the transitional bridge linking the nodes across the phenological stages, and to estimate the corresponding transition dates. The pheno-network model was utilized to represent the phenological progress of corn and soybean in Illinois from 2002 to 2017. With reference to the ASD-level ground phenological observations, the detected transition dates for corn were found to align with its mature stage. The R square was 0.55 and the RMSE was 7.77 days. As for soybean, the estimated transition dates corresponded to its dropping leaves stage, with the R square being 0.55 and the RMSE being 5.05 days. Compared to conventional phenological methods, the non-parametric pheno-network model does not make mathematical assumptions of crop phenological processes, and can be constructed with partial-year remote sensing data. The pheno-network model, with those unique characteristics, shows great promise to improve the phenological monitoring in complex and intensified agricultural systems.

Acknowledgements

This research is partially supported by NSF Office of Advanced Cyberinfrastructure award (1849821) and Campus Research Board (RB18146) at the University of Illinois at Urbana-Champaign. This research is also part of the Blue Waters sustained-petascale computing project, which is supported by the National Science Foundation (awards OCI-0725070 and ACI-1238993) and the state of Illinois. Blue Waters is a joint effort of the University of Illinois at Urbana-Champaign and its National Center for Supercomputing Applications.

References

Atkinson, P.M., Jeganathan, C., Dash, J., Atzberger, C., 2012. Inter-comparison of four models for smoothing satellite sensor time-series data to estimate vegetation phenology. Remote Sens. Environ. 123, 400–417.
Barabási, A.-L., 2009. Scale-free networks: a decade and beyond. Science 325, 412–413.

Beck, P.S.A., Atzberger, C., Høgda, K.A., Johansen, B., Skidmore, A.K., 2006. Improved monitoring of vegetation dynamics at very high latitudes: A new method using MODIS NDVI. Remote Sens. Environ. 100, 321–334.
Bolton, D.K., Friedl, M.A., 2013. Forecasting crop yield using remotely sensed vegetation indices and crop phenology metrics. Agric. For. Meteorol. 173, 74–84.
Boschetti, M., Stroppiana, D., Brivio, P.A., Bocchi, S., 2009. Multi-year monitoring of rice crop phenology through time series analysis of MODIS images. Int. J. Remote Sens. 30, 4643–4662.
Brockmann, D., Helbing, D., 2013. The hidden geometry of complex, network-driven contagion phenomena. Science 342, 1337–1342.
Brown, M.E., de Beurs, K.M., Marshall, M., 2012. Global phenological response to climate change in crop areas using satellite remote sensing of vegetation, humidity and temperature over 26years. Remote Sens. Environ. 126, 174–183.
Buldyrev, S.V., Parshani, R., Paul, G., Stanley, H.E., Havlin, S., 2010. Catastrophic cascade of failures in interdependent networks. Nature 464, 1025–1028.
Diao, C., Wang, L., 2014. Development of an invasive species distribution model with fine-resolution remote sensing. Int. J. Appl. Earth Observ. Geoinform. 30, 65–75.
Diao, C., Wang, L., 2016a. Incorporating plant phenological trajectory in exotic saltcedar detection with monthly time series of Landsat imagery. Remote Sens. Environ. 182, 60–71.
Diao, C., Wang, L., 2016b. Temporal partial unmixing of exotic salt cedar using Landsat time series. Remote Sens. Lett. 7, 466–475.
Diao, C., Wang, L., 2018. Landsat time series-based multiyear spectral angle clustering (MSAC) model to monitor the inter-annual leaf senescence of exotic saltcedar. Remote Sens. Environ. 209, 581–593.
Dong, J., Xiao, X., 2016. Evolution of regional to global paddy rice mapping methods: A review. ISPRS J. Photogramm. Remote Sens. 119, 214–227.
Eagle, N., Pentland, A.S., Lazer, D., 2009. Inferring friendship network structure by using mobile phone data. Proc. Natl. Acad. Sci. 106, 15274–15278.
Feng, G., Masek, J., Schwaller, M., Hall, F., 2006. On the blending of the Landsat and MODIS surface reflectance: predicting daily Landsat surface reflectance. IEEE Trans. Geosci. Remote Sens. 44, 2207–2218.
Foley, J.A., Levis, S., Costa, M.H., Cramer, W., Pollard, D., 2000. Incorporating dynamic vegetation cover within global climate models. Ecol. Appl. 10, 1620–1632.
Freeman, L.C., 1978. Centrality in social networks conceptual clarification. Social Networks 1, 215–239.
Gao, F., Anderson, M.C., Zhang, X., Yang, Z., Alfieri, J.G., Kustas, W.P., Mueller, R., Johnson, D.M., Prueger, J.H., 2017. Toward mapping crop progress at field scales through fusion of Landsat and MODIS imagery. Remote Sens. Environ. 188, 9–25.
Gómez, C., White, J.C., Wulder, M.A., 2016. Optical remotely sensed time series data for land cover classification: a review. ISPRS J. Photogramm. Remote Sens. 116, 55–72.
Hermance, J.F., Jacob, R.W., Bradley, B.A., Mustard, J.F., 2007. Extracting phenological signals from multiyear AVHRR NDVI time series: framework for applying high-order annual splines with roughness damping. IEEE Trans. Geosci. Remote Sens. 45, 3264–3276.
Jia, T., Qin, K., Shan, J., 2014. An exploratory analysis on the evolution of the US airport network. Phys. A: Statist. Mech. Appl. 413, 266–279.
Jin, Z., Azzari, G., Lobell, D.B., 2017. Improving the accuracy of satellite-based high-resolution yield estimation: A test of multiple scalable approaches. Agric. For. Meteorol. 247, 207–220.
Johnson, D.M., Mueller, R., 2010. The 2009 Cropland Data Layer. PE&RS, Photogramm. Eng. Remote Sens. 76, 1201–1205.
Jonsson, P., Eklundh, L., 2002. Seasonality extraction by function fitting to time-series of satellite sensor data. IEEE Trans. Geosci. Remote Sens. 40, 1824–1832.
Kilgore, G.L., Fjell, D., 1997. Soybean Production Handbook. Publication C-449, Kansas State University Agricultural Experiment Station and Cooperative Extension Service, Manhattan, Kansas, pp. 8–9.
Kramer, K., Leinonen, I., Loustau, D., 2000. The importance of phenology for the evaluation of impact of climate change on growth of boreal, temperate and Mediterranean forests ecosystems: an overview. Int. J. Biometeorol. 44, 67–75.
Kucharik, C.J., 2006. A multidecadal trend of earlier corn planting in the Central USA. Agron. J. 98, 1544–1550.
Lauer, J., 2012. The effects of drought and poor corn pollination on corn. Field Crops 28, 493–495.
Lehecka, G.V., 2014. The value of USDA crop progress and condition information: Reactions of corn and soybean futures markets. J. Agric. Resour. Econ. 88–105.
Lieth, H., 2013. Phenology and Seasonality Modeling. Springer Science & Business Media.
Liu, Z., Wu, C., Liu, Y., Wang, X., Fang, B., Yuan, W., Ge, Q., 2017. Spring green-up date derived from GIMMS3g and SPOT-VGT NDVI of winter wheat cropland in the North China Plain. ISPRS J. Photogramm. Remote Sens. 130, 81–91.
Lobell, D.B., Thau, D., Seifert, C., Engle, E., Little, B., 2015. A scalable satellite-based crop yield mapper. Remote Sens. Environ. 164, 324–333.
MacBean, N., Maignan, F., Peylin, P., Bacour, C., Bréon, F.M., Ciais, P., 2015. Using satellite data to improve the leaf phenology of a global terrestrial biosphere model. Biogeosciences 12, 7185–7208.
Manfron, G., Delmotte, S., Busetto, L., Hossard, L., Ranghetti, L., Brivio, P.A., Boschetti, M., 2017. Estimating inter-annual variability in winter wheat sowing dates from satellite time series in Camargue, France. Int. J. Appl. Earth Observ. Geoinform. 57, 190–201.
Moreira, A., Fontana, D.C., Kuplich, T.M., 2019. Wavelet approach applied to EVI/MODIS time series and meteorological data. ISPRS J. Photogramm. Remote Sens. 147, 335–344.
Morisette, J.T., Richardson, A.D., Knapp, A.K., Fisher, J.I., Graham, E.A., Abatzoglou, J., Wilson, B.E., Breshears, D.D., Henebry, G.M., Hanes, J.M., Liang, L., 2008. Tracking the rhythm of the seasons in the face of global change: phenological research in the 21st century. Front. Ecol. Environ. 7, 253–260.
Newman, M., Barabasi, A.-L., Watts, D.J., 2011. The Structure and Dynamics of Networks. Princeton University Press.
Newman, M.E.J., 2010. Networks: An Introduction. Oxford University Press, Oxford.
Peng, D., Zhang, X., Zhang, B., Liu, L., Liu, X., Huete, A.R., Huang, W., Wang, S., Luo, S., Zhang, X., Zhang, H., 2017. Scaling effects on spring phenology detections from MODIS data at multiple spatial resolutions over the contiguous United States. ISPRS J. Photogramm. Remote Sens. 132, 185–198.
Peñuelas, J., Filella, I., 2001. Responses to a Warming World. Science 294, 793.
Qin, Y., Xiao, X., Dong, J., Zhou, Y., Zhu, Z., Zhang, G., Du, G., Jin, C., Kou, W., Wang, J., Li, X., 2015. Mapping paddy rice planting area in cold temperate climate region through analysis of time series Landsat 8 (OLI), Landsat 7 (ETM+) and MODIS imagery. ISPRS J. Photogramm. Remote Sens. 105, 220–233.
Richardson, A.D., Anderson, R.S., Arain, M.A., Barr, A.G., Bohrer, G., Chen, G., Chen, J.M., Ciais, P., Davis, K.J., Desai, A.R., Dietze, M.C., Dragoni, D., Garrity, S.R., Gough, C.M., Grant, R., Hollinger, D.Y., Margolis, H.A., McCaughey, H., Migliavacca, M., Monson, R.K., Munger, J.W., Poulter, B., Raczka, B.M., Ricciuto, D.M., Sahoo, A.K., Schaefer, K., Tian, H., Vargas, R., Verbeeck, H., Xiao, J., Xue, Y., 2012. Terrestrial biosphere models need better representation of vegetation phenology: results from the North American Carbon Program Site Synthesis. Glob. Change Biol. 18, 566–584.
Richardson, A.D., Hufkens, K., Milliman, T., Aubrecht, D.M., Chen, M., Gray, J.M., Johnston, M.R., Keenan, T.F., Klosterman, S.T., Kosmala, M., Melaas, E.K., Friedl, M.A., Frolking, S., 2018. Tracking vegetation phenology across diverse North American biomes using PhenoCam imagery. Sci. Data 5, 180028.
Richardson, A.D., Keenan, T.F., Migliavacca, M., Ryu, Y., Sonnentag, O., Toomey, M., 2013. Climate change, phenology, and phenological control of vegetation feedbacks to the climate system. Agric. For. Meteorol. 169, 156–173.
Rubinov, M., Sporns, O., 2010. Complex network measures of brain connectivity: Uses and interpretations. NeuroImage 52, 1059–1069.
Sakamoto, T., 2018. Refined shape model fitting methods for detecting various types of phenological information on major U.S. crops. ISPRS J. Photogramm. Remote Sens. 138, 176–192.
Sakamoto, T., Gitelson, A.A., Arkebauer, T.J., 2013. MODIS-based corn grain yield estimation model incorporating crop phenology information. Remote Sens. Environ. 131, 215–231.
Sakamoto, T., Wardlow, B.D., Gitelson, A.A., Verma, S.B., Suyker, A.E., Arkebauer, T.J., 2010. A Two-Step Filtering approach for detecting maize and soybean phenology with time-series MODIS data. Remote Sens. Environ. 114, 2146–2159.
Sakamoto, T., Yokozawa, M., Toritani, H., Shibayama, M., Ishitsuka, N., Ohno, H., 2005. A crop phenology detection method using time-series MODIS data. Remote Sens. Environ. 96, 366–374.
Tornos, L., Huesca, M., Dominguez, J.A., Moyano, M.C., Cicuendez, V., Recuero, L., Palacios-Orueta, A., 2015. Assessment of MODIS spectral indices for determining rice paddy agricultural practices and hydroperiod. ISPRS J. Photogramm. Remote Sens. 101, 110–124.
Walthall, C.L., Anderson, C.J., Baumgard, L.H., Takle, E., Wright-Morton, L., 2013. Climate change and agriculture in the United States: Effects and adaptation.
Wang, C., Fan, Q., Li, Q., SooHoo, W.M., Lu, L., 2017. Energy crop mapping with enhanced TM/MODIS time series in the BCAP agricultural lands. ISPRS J. Photogramm. Remote Sens. 124, 133–143.
Wardlow, B.D., Kastens, J.H., Egbert, S.L., 2006. Using USDA Crop Progress Data for the Evaluation of Greenup Onset Date Calculated from MODIS 250-Meter Data. Photogramm. Eng. Remote Sens. 72, 1225–1234.
Watts, D.J., Strogatz, S.H., 1998. Collective dynamics of small-world networks. Nature 393, 440–442.
White, M.A., Thornton, P.E., Running, S.W., 1997. A continental phenology model for monitoring vegetation responses to interannual climatic variability. Global Biogeochem. Cycles 11, 217–234.
Wu, J., Zhou, L., Liu, M., Zhang, J., Leng, S., Diao, C., 2013. Establishing and assessing the Integrated Surface Drought Index (ISDI) for agricultural drought monitoring in mid-eastern China. Int. J. Appl. Earth Observ. Geoinform. 23, 397–410.
Zhang, X., Friedl, M.A., Schaaf, C.B., 2006. Global vegetation phenology from Moderate Resolution Imaging Spectroradiometer (MODIS): Evaluation of global patterns and comparison with in situ measurements. J. Geophys. Res.: Biogeosci. 111.
Zhang, X., Friedl, M.A., Schaaf, C.B., Strahler, A.H., Hodges, J.C.F., Gao, F., Reed, B.C., Huete, A., 2003. Monitoring vegetation phenology using MODIS. Remote Sens. Environ. 84, 471–475.
Zhang, X., Zhang, Q., 2016. Monitoring interannual variation in global crop yield using long-term AVHRR and MODIS observations. ISPRS J. Photogramm. Remote Sens. 114, 191–205.
Zhong, L., Hu, L., Yu, L., Gong, P., Biging, G.S., 2016. Automated mapping of soybean and corn using phenology. ISPRS J. Photogramm. Remote Sens. 119, 151–164.
Zhou, L., Wu, J., Mo, X., Zhou, H., Diao, C., Wang, Q., Chen, Y., Zhang, F., 2017. Quantitative and detailed spatiotemporal patterns of drought in China during 2001–2013. Sci. Total Environ. 589, 136–145.